

# Analysis of the Key Elements on the 2-D Electro-optic Modulation of BaTiO<sub>3</sub> Crystal Thin-film Waveguide

Mengxi Luo, Degui Sun\* and Na Sun

School of Science, Changchun University of Science and Technology 7089 Weixing Road, Changchun JL, China

\*Corresponding author

**Abstract**—As ferroelectric crystal, barium titanate (BTO) crystal with an ultra-high electro-optical (EO) coefficient and a special modulation mechanism has become the most popular research object to realize the ultra-high bandwidth EO modulator (over 100GHz). In this paper, we model/simulate the conditions of two different kinds of EO modulation for the a- and c-axis grown BTO crystal thin-films through a new embedded waveguide-electrode structure. As a result, the mutual influences between the microwave electric-field and the light field in determining the optimal interaction overlap integral are found to determine the highest modulation efficiency. Meanwhile, we also see the influence of the BTO birefringence on the modulation efficiencies of the two different orientations of BTO crystal films. Under the optimized conditions, the device designs have the better performance and the more accurate electro-optical coefficient. It can be seen from the simulated data in this paper that under the quasi-linear electro-optical modulation of a-axis, when the optical axis and waveguide transmission direction are at a 45-degree angle, the EO interaction effect of the new embedded waveguide electrode structure is realized, and then the highest EO modulation is reached, which is about 1.47V·mm. In contrast, under the nonlinear modulation of c-axis, where a perpendicular electric field to the axis of BTO crystal is applied and then it reaches the lowest V<sub>π</sub>·L performance of 4.38V<sup>2</sup>·mm.

**Keywords**—barium titanate; coefficient; birefringence; refractive index variation; electro-optical modulation; embedded

## I. INTRODUCTION

In recent years, the rapid development of optical communication technology has placed higher requirements on the capacity and speed of electro-optic (EO) modulators [1-3]. The single-channel modulation bandwidth of optical modulators must be increased from the current 10-40GHz to more than 100GHz to meet the requirements. And at this stage the lithium niobate crystal waveguide based EO modulators and semiconductor electric absorption (EA) optical modulators can satisfy this requirement, but the highest bandwidth is only 40 GHz that has reached its maximum potential [4-7]. Due to its special physical properties of BTO - ultra high EO coefficient, special EO modulation, can achieve compatible with silicon photonic waveguide devices and integration advantages, such as EO modulator can achieve low voltage high bandwidth to become a research focus at present stage, based on barium titanate crystal thin film waveguide EO modulator will occupy the important position in the next generation optical network.

## II. ELECTRO-OPTIC MODULATION MODEL

### A. The Theory of EO Modulation

The first modulation scheme is a quasi-linear modulation with a mixed effect of two EO coefficients r<sub>51</sub> and r<sub>31</sub> by optimizing an angle of electric field and the second modulation scheme is a cross-modulation term of single EO coefficient — r<sub>51</sub>. Figure I(a) schematically shows an angled EO modulation to a c-axis grown BaTiO<sub>3</sub> crystal thin-film waveguide. We know the general EO modulation of a ferroelectric crystal is defined as

$$\left(\frac{1}{n_o^2} + r_{13}E_z\right)x^2 + \left(\frac{1}{n_o^2} + r_{13}E_z\right)y^2 + \left(\frac{1}{n_e^2} + r_{33}E_x\right)z^2 + (r_{51}E_y)2yz + (r_{51}E_x)2zx = 1 \quad (1)$$

For the case of angled EO modulation as shown in Figure I(a), the coordinate transformation of effective refractive index can be obtained as Eq. (2) and the relation of the half-wave voltage and the operating length can be obtained as Eq. (3):

$$\Delta n_{eff}(\phi) = \frac{n_{eff}^3(\phi)r_{eff}\Gamma_x(\phi)}{2G(\phi)} \cdot V(\phi) \quad (2)$$

$$V_{\pi}(\phi) \cdot L = \frac{\lambda G(\phi)}{n_{eff}^3(\phi)r_{eff}\Gamma_{TE}(\phi)} \quad (3)$$

To the contrast, for the case of parallel EO modulation as shown in Figure I(b), we can directly obtain a new form of optical refractive index modulation model and the relationship between the half-wave voltage and the operating length as

$$V_{\pi}^2 L = \frac{\lambda \left[ \frac{1}{n_e^2} - \frac{1}{n_o^2} \right]}{\left( n_e^3 + n_o^3 \right) \times \left( \frac{\Gamma_x}{G_x} r_{51} \right)^2} \quad (4)$$

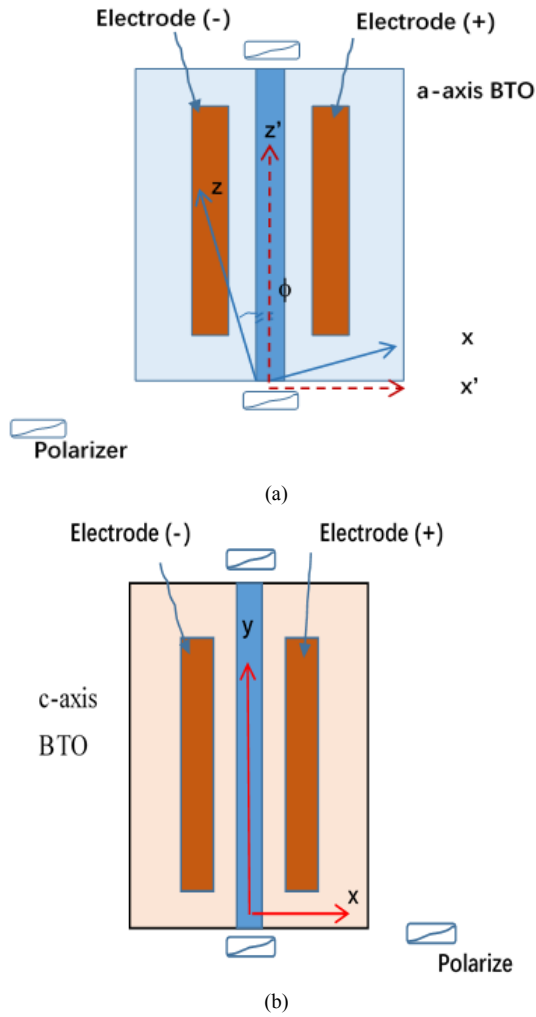


FIGURE I. SCHEMATIC DIAGRAM OF ELECTRO-OPTICAL MODULATION OF WAVEGUIDE IN DIFFERENT AXIAL BARIUM TITANATE CRYSTAL THIN FILM(A)A-AXIS;(B)C-AXIS

### III. SIMULATIONS FOR EO MODULATION CHARACTERISTICS OF BTO CRYSTAL

#### A. The Modulation Efficiency

In previous studies, the modulation efficiency of barium titanate crystal film waveguide electrode can reach 0.65.[8]We use the 2D matching because of the embedded structure,the modulation efficiency is higher.As shown in the Figure II, with the change of electrode sinking depth, the whole BTO waveguide electrode, the modulation efficiency curve.(5) is the overlap integral in embedded waveguide electrode structure under two-dimensional electro-optical action.

$$\Gamma_{2D} = \frac{G_x}{V} \frac{\iint E(x, z - S_z) |E_{opt}(x, z)|^2 dx dz}{\iint |E_{opt}(x, z)|^2 dx dz} \quad (5)$$

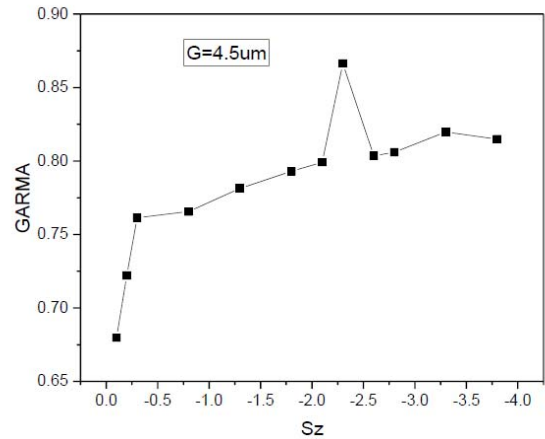


FIGURE II. AT AN ELECTRODE GAP  $G_x=4.5\mu\text{m}$ , THE RELATIONSHIP BETWEEN THE OVERLAP INTEGRAL OF THE ELECTRIC-OPTICAL FIELD IN BARIUM TITANATE CRYSTAL THIN FILM WAVEGUIDE AND THE SINKING DEPTH, WHERE THE WIDTH AND THICKNESS OF ELECTRODES ARE  $W=10\text{mm}$ ,  $T=5\text{mm}$ , RESPECTIVELY; THE WIDTH AND HEIGHT OF WAVEGUIDES ARE  $W=3.0\text{mm}$ ,  $H=0.2\text{mm}$ , RESPECTIVELY

It can be seen from Figure II that the EO modulation efficiency increases gradually from  $0.1\mu\text{m}$  to  $2.3\mu\text{m}$  with the upper surface of barium titanate as the zero potential surface, and the maximum modulation efficiency can be up to 0.88, indicating that the intensity distribution of electric field matches the intensity distribution of optical field, the interaction intensity is the maximum, and the modulation efficiency is the highest. Thereby, by setting the sinking depth  $S_z=2.3\mu\text{m}$ , with Eq. (5) we simulate the electric-optic field overlap integral  $\Gamma$  dependences on the electrode gap  $G$  for the traditional co-planar waveguide (CPW) modulation scheme and the embedded waveguide scheme shown in Figure I(a) and I(b), respectively, with respect to three different values of waveguide width. Note from Figure III(a) that for the CPW scheme, the two smaller width values  $2.0$  and  $3.0\mu\text{m}$ : the  $\Gamma_{1D}$  value increases with  $G$ , but for the larger waveguide width  $4.0\mu\text{m}$ , the  $\Gamma_{1D}$  maintains at the extremely high values and independent of  $G$  value. In contrast, Note from Figure III(b) that for the embedded scheme, for all the three waveguide widths, the  $\Gamma_{1D}$  value decreases with  $G$ . Namely, the overlap integral increases with the electric field strength applied.

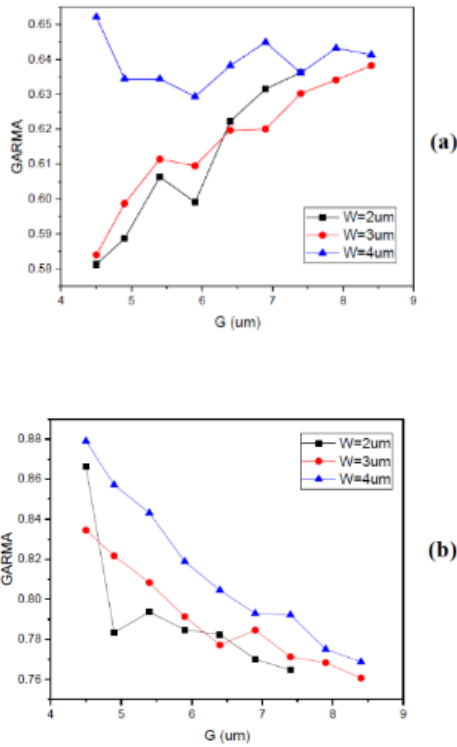


FIGURE III. SIMULATIONS OF WIDTH CONDITIONS, THE RELATIONSHIP BETWEEN THE MODULATION EFFICIENCY AND THE ELECTRODE GAP UNDER TWO STRUCTURES. (A) CPW AND (B) THE EMBEDDED

**B. Birefringence**

Due to the anisotropy of barium titanate crystal, the refractive indices of o light and e light should be modulated at the same time. Therefore, the birefringence should be considered into the theoretical model of this paper to improve the efficiencies of EO modulation. Figure IV shows the variation of refractive index ellipsoid barium titanate crystal when an electric-field  $E_x$  is applied at x-direction. Note that the variation of the refractive index ellipsoid involves both the length and direction of the long axis.

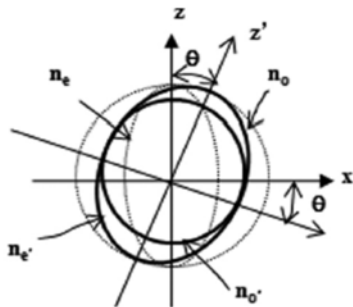


FIGURE IV. THE REFRACTIVE INDEX ELLIPSOID CHANGE DRIVEN BY E-FIELD  $E_x$ , WHERE THE CIRCLES AND ELLIPSES OF DOTTED LINES ARE THE STATES BEFORE THE E-FIELD IS APPLIED, AND THE SOLID LINES REPRESENT THE STATES AFTER THE ELECTRIC FIELD IS APPLIED

In this paper, by setting  $r_{51}=500\text{pm/V}$ ,  $r_{31}=28\text{pm/V}$ ,  $r_{13}=8\text{pm/V}$ , the wavelength  $\lambda=1550\text{nm}$ , the waveguide rib  $W=4\mu\text{m}$ ,  $H=0.2\mu\text{m}$ ,  $S_z=2.3\mu\text{m}$ , then with Eq. (2) we first obtain the relationship between the effective coefficient  $r_{\text{eff}}$  and the electrode gap with respect to three values of angle  $\phi$  as shown in Figure V. As an illustration, note that when the electrode gap is  $4.5\mu\text{m}$ ,  $V_\pi$  is  $5\text{V}$ , for  $\phi=45^\circ$ , in the CPW structure, the refractive index modulation is  $5.70 \times 10^{-3}$ , while the refractive index modulation in the embedded model is  $7.85 \times 10^{-3}$ , the refractive index modulation of the later is higher than that of the former by 38%. For  $\phi=35^\circ$ , the refractive index modulations are  $4.5 \times 10^{-3}$  and  $6.1 \times 10^{-3}$  in the CPW structure and the embedded structure, respectively, then the refractive index modulation of the later is higher than that of the former by 36%. In Castera's work [9], when the angle is  $35^\circ$ , quasi-linear EO modulation is considered to be the best, but in this paper, as shown in Figure V our work simulations for the relationship between the refractive index modulation and the electrode gap  $G$  has shown a new discovery with the quasi-linear EO modulation model. In this discovery, under the condition of embedded model and when the angle is  $45^\circ$  the refractive index modulation  $\Delta n$  has higher value that at  $35^\circ$  for the same  $G$  value. At this point, we simulate the relationship between  $V_\pi L$  and  $G$  with respect to three  $\phi$  values, then also find  $V_\pi L$  has the lowest value of  $1.47\text{V}\cdot\text{mm}$ , so the EO modulation is the best state.

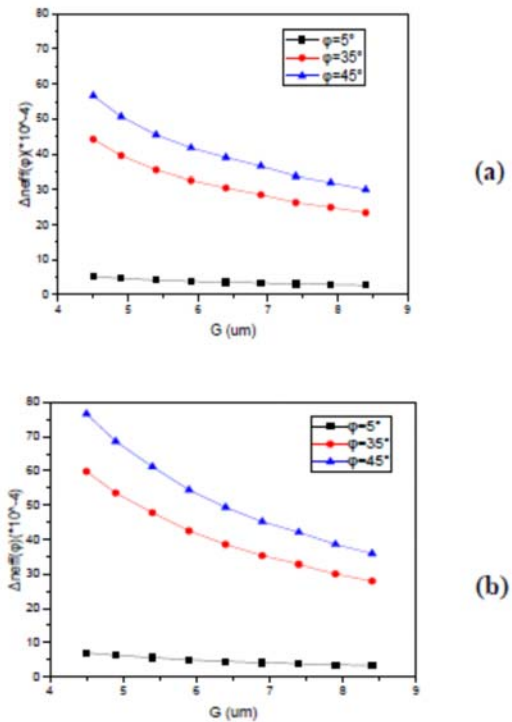


FIGURE V. THE RELATIONSHIP BETWEEN THE REFRACTIVE INDEX MODULATION AND THE ELECTRODE GAP WITH RESPECT TO THREE VALUES: (A) THE CPW SCHEME AND (B) THE EMBEDDED SCHEME.

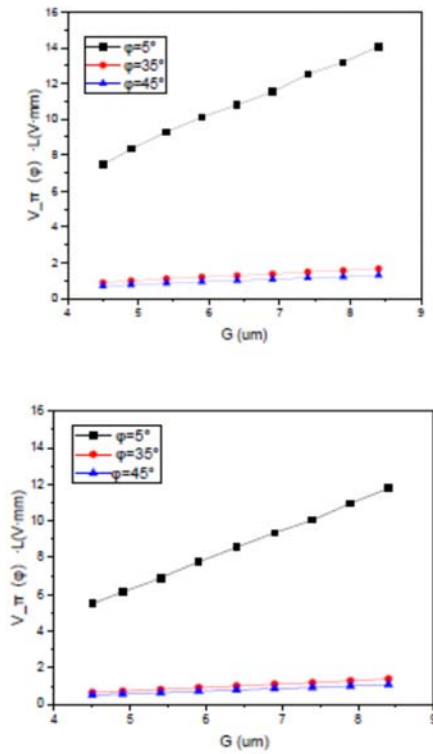


FIGURE VI. THE RELATIONSHIP BETWEEN  $V_{\pi}^2 L$  AND ELECTRODE GAP WITH RESPECT TO THREE VALUES: (A) THE CPW SCHEME AND (B) THE EMBEDDED SCHEME

In contrast with the quasi-linear EO modulation model defined by Eq. (3), we investigate the refractive index modulation effects of barium titanate crystal thin film waveguide EO modulator with the nonlinear EO modulation model defined by Eq. (3). With the nonlinear EO modulation model, we also simulate the relationship between the  $V_{\pi}^2 L$  and the electrode gap  $G$  for both the CPW and the embedded scheme under the different birefringence conditions as shown in Figure VII. Note that with the decrease of birefringence value and the electrode gap decreases,  $V_{\pi}^2 L$  decrease. Then, we can conclude that the birefringence plays an important role in refractive index modulation. In addition, for the same birefringence value, the embedded scheme has a much lower  $V_{\pi}^2 L$  value than the CPW scheme. For instance, when the electrode gap is  $4.5\mu\text{m}$ ,  $V_{\pi}$  is  $5\text{V}$ ,  $\text{beo} = -0.005$ , in the case of the CPW scheme, the  $V_{\pi}^2 L$  has the value of  $21.0\text{V}^2\cdot\text{mm}$ , in contrast in the embedded scheme, it is only  $11.5\text{V}^2\cdot\text{mm}$ . Thus, we can obtain the  $V_{\pi}^2 L$  value of the embedded scheme is only the 0.55 of that of the CPW. Such a difference of  $V_{\pi}^2 L$  value can lead to a different interaction length  $L$  when a  $V_{\pi}$  is given. Here,  $V_{\pi}$  is set as  $5\text{V}$ , so  $L$  has the values of  $0.84$  and  $0.46\text{mm}$ , respectively. As shown in our previous work, the shorter interaction length  $L$  is sustainable to improve the bandwidth of EO modulators [3-5].

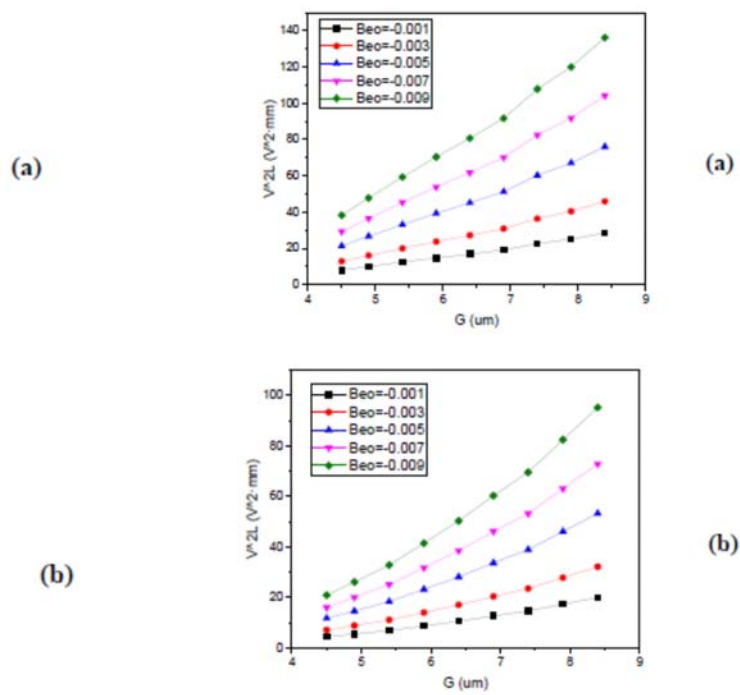


FIGURE VII. THE RELATIONSHIP BETWEEN THE  $V_{\pi}^2 L$  AND THE ELECTRODE GAP UNDER THE DIFFERENT BIREFRINGENCE CONDITIONS: (A) THE CPW SCHEME AND (B) THE EMBEDDED SCHEME

#### IV. CONCLUSIONS

With the analyzing theories of EO modulation characteristics of  $\text{BaTiO}_3$  crystal, the key elements on the 2-D EO modulation of  $\text{BaTiO}_3$  crystal thin-film waveguide are very important to realize the highly efficient EO modulations. We have obtained a new type of embedded waveguide electrode structure, and then improved the performance of the structure. By studying the important parameters of barium titanate crystal, both the theoretical models of linear and nonlinear EO modulation are improved. At the same time, a new discovery in the study of linear EO modulation is that when the angle is  $45^\circ$ , its EO modulation performance is the best. The angle between the optical axis and the beam transmission direction in quasi-linear EO modulation is compared and determined. In this paper, we find that the influence of two important parameters on EO modulation are modulation efficiency and birefringence.

#### ACKNOWLEDGMENT

This work is sponsored by the Department of Science and Technology of Jilin Provincial Fund (20160101263JC).

#### REFERENCES

- [1] Saleh, A. A. A. M. and J. M. Simmons, "Evolution toward the next-generation core optical networks" *J. Lightwave Technol.*, Vol. 24, No. 9, 3303–3321, 2006.
- [2] Yamazaki, H., T. Saida, T. Goh, S. Mino, M. Nagatani, H. Nosaka, and K. Murata, "Dualcarrier dual-polarization IQ modulator using complementary frequency shifter" *IEEE J. Sel. Top. Quan. Electron.*, Vol. 19, No. 6, 3400208, 2013.

- [3] Sun, D. G., J. Zhang, C. Chen, M. Kong, J. Wang, and H. Jiang, "Theoretical feasibility for over 100 GHz electro-optic modulators with c-axis grown BaTiO<sub>3</sub> crystal thin-films" *J. Lightwave Technol.*, Vol. 33, No. 10, 1937–1947, 2015.
- [4] Wooten, E. L., K. M. Kissa, A. Yi-Yan, E. J. Murphy, D. A. Lafaw, P. F. Hallemeier, D. Maack, D. V. Attanasio, D. J. Tritz, G. J. McBrien, and D. E. Bossi, "A review of lithium niobite modulators for fiber-optic communications systems" *IEEE J. Sel. Top. Quantum Electron.*, Vol. 6, No. 1, 69–82, 2000.
- [5] Rahman, B. M. A. and S. Haxha, "Optimization of microwave properties for ultrahigh-speed etched and unetched lithium niobate electrooptic modulators" *J. Lightwave Technol.*, Vol. 20, No. 10, 1856–1863, 2002.
- [6] Li, G. L. and P. K. L. Yu, "Optical intensity modulators for digital and analog applications" *J. Lightwave Technol.*, Vol. 21, No. 9, 2010–2030, 2003.
- [7] Wülbern, J. H., S. Provok, J. Hampe, A. Petrov, M. Eich, J. D. Luo, A. K. Y. Jen, M. Jennett, and A. Jacob, "40 GHz electrooptic modulation in hybrid silicon-organic slotted photonic crystal waveguides" *Opt. Lett.*, Vol. 35, No. 16, 2753–2755, 2010.
- [8] Mengxi.Luo, Degui Sun, "Ultra-efficient modulation of BaTiO<sub>3</sub> crystal thin film waveguide with a two-dimensional optic-electric field matching scheme" *Journal of Applied Physics*, 123, 034503, 2018.
- [9] Pau Castera, Domenico Tulli, Ana M. Gutierrez, and Pablo Sanchis, "Influence of BaTiO<sub>3</sub> ferroelectric orientation for electro-optic modulation on silicon" *Optics express*, 23, 15332-15342, 2015.